ELSEVIER

Catalysis Today 33 (1997) 279–290

CATALYSIS TODAY

Effect of Cu loading and addition of modifiers on the stability of Cu/ZSM-5 in lean NO_x reduction catalysis

J.Y. Yan, W.M.H. Sachtler, H.H. Kung *

V.N. Ipatieff Laboratory, Department of Chemistry, Center for Catalysis and Surface Science, Northwestern University, Evanston, IL 60208, USA

Abstract

The stability of Cu/ZSM-5 catalysts of different Cu loadings or modified by addition of Na, La, or Ce was studied in lean NO_x reduction. Samples were characterized by H_2-TPR, EPR and XRD before and after deactivation. Increasing the Cu loading above 68% of the exchange capacity improved the stability, as did La addition, presumably because these decreased the concentration of protons which were instrumental in the dealumination of the ZSM-5 framework. Addition of Ce had little effect, because CeO_2 was formed and thus did not compete with protons for exchange sites. Addition of Na decreased the stability, because it promoted the formation of inactive CuO particles; in addition, migration of Cu^{2+} to a different coordination environment also seemed to contribute to the catalyst deactivation.

Keywords: Cu/ZSM-5; Deactivation; Dealumination; Stabilization ; Modification

1. Introduction

Since the first reports by Iwamoto et al. [1] and Held et al. [2] that Cu/ZSM-5 is active for selective lean NO_x reduction to N_2 by hydrocarbons, catalysts of this type have been studied extensively. It is known now that they deactivate rapidly under lean NO_x reduction conditions, i.e. in an atmosphere containing a high concentration of steam at a temperature of 400–800°C [3–9]. From our previous studies on the deactivation of these catalysts [9], it was concluded that dealumination of the zeolite framework, formation of amorphous Al_2O_3 and inactive Cu/Al_2O_3 contribute to the deactivation of the catalyst. It was also suggested that the presence of zeolite protons is crucial for dealumination and deactivation. In view of the potential technological importance of Cu/ZSM-5 catalyst, we investigated the effect of catalyst modification by a variety of cations on its stability. The modifiers studied include La^{3+}, Na^+ and Ce^{3+}. The effect of Cu^{2+} loading was also investigated. Catalysts were characterized in their active and deactivated states by temperature programmed reduction with H_2 (H_2-TPR), electron paramagnetic resonance spectroscopy (EPR) and X-ray diffraction spectroscopy (XRD). This paper reports the results of the investigation which further clarified the deactivation mechanism of Cu/ZSM-5.

* Corresponding author. Tel.: (708)491-7492; FAX: (708)467-1018; E-mail: hkung@nwu.edu.

PII S0920-5861(96)00100-9

2. Experimental

2.1. Materials

Cu/ZSM-5 samples were prepared by ion exchange at 25°C using a solution of $Cu(CH_3COO)_2$ (Aldrich) and Na/ZSM-5 (UOP) at pH = 5.5–6, following the method of Iwamoto et al. [10]. The chemical compositions of the samples (Table 1) were determined by inductive-coupled plasma atomic emission spectroscopy (ICP-AES) with an Atomscan 25 spectrometer (Thermal Jarrel Ash Corp.). The samples are labelled Cu/ZSM-5-(Si/Al ratio)-(percentage exchange).

Cation modified samples were prepared by impregnating an aqueous solution of $Na_2C_2O_4$ (Johnson-Mathey), $Ce(NO_3)_3$ (Aldrich), or $La(NO_3)_3$ (Aldrich) onto Cu/ZSM-5-17-102. The concentrations of the second cation were adjusted to obtain the desired M/Al ratio of 0.5 (Table 2). The samples are labelled Cu/M-(M/Al ratio)/ZSM-5.

2.2. Apparatus and procedure

Fresh samples of Cu/ZSM-5 or Cu/M/ZSM-5 were used for each catalytic test. The catalytic activities were measured at 400°C at 0.1 MPa in the absence of added water in a flow of NO (1000 ppm), C_3H_8 (1000 ppm), O_2 (2%), balanced with He. The total flow rate was 400 ml/min (which gave a GHSV about 120000 h^{-1}). The products were analyzed by GC equipped with a Porapak Q and a 5A molecular sieves column. CO_2 was the only carbon product detected. For the data reported

$$\text{NO conversion}\,\% = (2N_2/NO_{in}) \times 100\%$$

$$C_3H_8\ \text{conversion}\,\% = [CO_2/(3C_3H_{8,in})] \times 100\%$$

NO competitiveness factor

$$= [(2N_2)/(10 \times C_3H_{8,consumed})] \times 100\%$$

The NO competitiveness factor is the percentage of the consumed hydrocarbon which is used for the reduction of NO.

Deactivation was carried out in the presence of added water in a flow of NO (1000 ppm), C_3H_8 (1000 ppm), O_2 (2%), H_2O (10%), balanced with He. In order to deactivate the samples in a reasonable time, deactivation was carried out at 500°C. At this temperature, there was no thermal degradation of the samples. The deactivation time varied for different catalysts, and was chosen to yield about 60% loss of N_2 production activity.

Temperature-programmed reduction (TPR) was carried out using H_2/Ar (5%) as reductant (flow rate = 30 ml/min), starting from −48°C with a heating rate of 8°C/min. A thermal conductivity cell was used to monitor the H_2 consumption. The amount of H_2 consumed was calibrated using a $CuO + SiO_2$ mixture as standard. The samples were first calcined in O_2 at 500°C for at least 2 h and cooled in O_2 to −80°C, then purged with Ar (30 ml/min) for 1 h and with H_2/Ar (30 ml/min) for 1 h at −80°C before TPR runs.

Electron paramagnetic resonance (EPR) data were collected at 77 K with a Varian E-4 spectrometer. After the desired pretreatments, the samples were calcined in O_2 at 500°C for 2 h.

Table 1
Composition of Cu/ZSM-5 samples

Sample	Si/Al	Na/Al	Cu/Al	Exchange level (%)	Cu (wt%)
Cu/ZSM-5-17-68	17	0.11	0.34	68	1.84
Cu/ZSM-5-17-102	17	0.03	0.51	102	2.43
Cu/ZSM-5-18-113	18	0.02	0.57	113	2.73

Table 2
Composition of Cu/M/ZSM-5-17-102 samples

Sample	M	M/Al	M (wt%)
Cu/Na-0.5/ZSM-5-17-102	Na	0.5	0.9
Cu/Ce-0.5/ZSM-5-17-102	Ce	0.53	6.5
Cu/La-0.5/ZSM-5-17-102	La	0.53	6.5

After purging the cell with Ar and evacuation at room temperature, the samples were transferred to the EPR sample tubes and sealed under vacuum without exposure to air.

Powder XRD data were collected in air with a Rigaku diffractometer, using Cu K_α radiation and a Ni filter.

3. Results

3.1. Cu / ZSM-5

The catalytic activities of the three Cu/ZSM-5 catalysts before and after deactivation treatments are listed in Table 3. It can be seen that the deactivation rates of the three catalysts were quite different, being slower for samples of higher copper loadings. The competitiveness factors increased substantially upon deactivation.

The TPR profiles of fresh Cu/ZSM-5 samples are shown in Fig. 1A. The profiles of Cu/ZSM-5-17-102 (curve b) and Cu/ZSM-5-18-113 (curve c) show three H_2-consumption peaks at 15°C, 150–200°C, and > 250°C. They have been assigned to the reduction of $[Cu\text{-}O\text{-}Cu]^{2+}$ to 2 Cu^+, Cu^{2+} to Cu^+, and Cu^+ to Cu^0, respectively [9]. With increasing copper loading, the peak of Cu^+ reduction to Cu° shifted to a lower temperature. This reflects the autocatalytic nature of this reduction; presence of Cu^0 accelerates the reduction rate and a lower temperature is required [9]. Only two peaks were visible in the TPR profile of Cu/ZSM-5-17-68 (curve a), in agreement with earlier findings that little or no $[Cu\text{-}O\text{-}Cu]^{2+}$ oxocations were present at low Cu loading [11]. The peak at −20°C was an artifact caused by Ar desorption.

The TPR profiles of deactivated Cu/ZSM-5 samples are shown in Fig. 1B. In comparison to the fresh samples, the following changes are noted: (a) The peak at 15°C disappeared, suggesting loss of $[Cu\text{-}O\text{-}Cu]^{2+}$ in the deactivated samples. (b) A broad peak appeared, which began at about 160°C, and extended to high temperature. This broad feature has been assigned to Cu dispersed in or on Al_2O_3 [9]. (c) The high temperature peak was shifted to high temperatures. (d) In the Cu/ZSM-5-18-113 sample, a new broad peak appeared above 400°C. This broad feature has been assigned to the reduction of $CuAl_2O_4$ [9]. The ratio of H_2 consumed to Cu was unity for Cu/ZSM-5-17-68 and Cu/ZSM-5-17-102, but 0.92 for Cu/ZSM-5-18-113, suggesting that reduction of the latter sample was not complete at the end of TPR experiment (500°C).

The EPR spectra of fresh and deactivated Cu/ZSM-5 samples are shown in Fig. 2A and Fig. 2B. The spectra of all three fresh samples showed only one type of Cu^{2+} ions with $A_{\|}$ = 154 G and $g_{\|} = 2.30$. The spectra of the deactivated samples showed two types of Cu^{2+} ions, one of which, with $A_{\|} = 148$ G and $g_{\|} = 2.31$, was likely the same species as that detected in the fresh samples. The other, with $A_{\|} = 174$ G

Table 3
Catalytic activities of Cu/ZSM-5 samples [a]

Sample	Fresh			Deactivation time (h) [b]	Deactivated		
	NO conversion to N_2 (%)	C_3H_8 conversion (%)	Competitiveness factor (%)		NO conversion to N_2 (%)	C_3H_8 conversion (%)	Competitiveness factor (%)
Cu/ZSM-5-17-68	53	92	5.8	6	18	13	10.6
Cu/ZSM-5-17-102	49	92	5.3	21	18	23	7.8
Cu/ZSM-5-18-113	60	98	6.1	46	31	36	8.6

[a] Activities were obtained under dry catalysis conditions at 400°C (see Experimental).
[b] Time of deactivation conducted under wet catalysis conditions at 500°C (see Experimental).

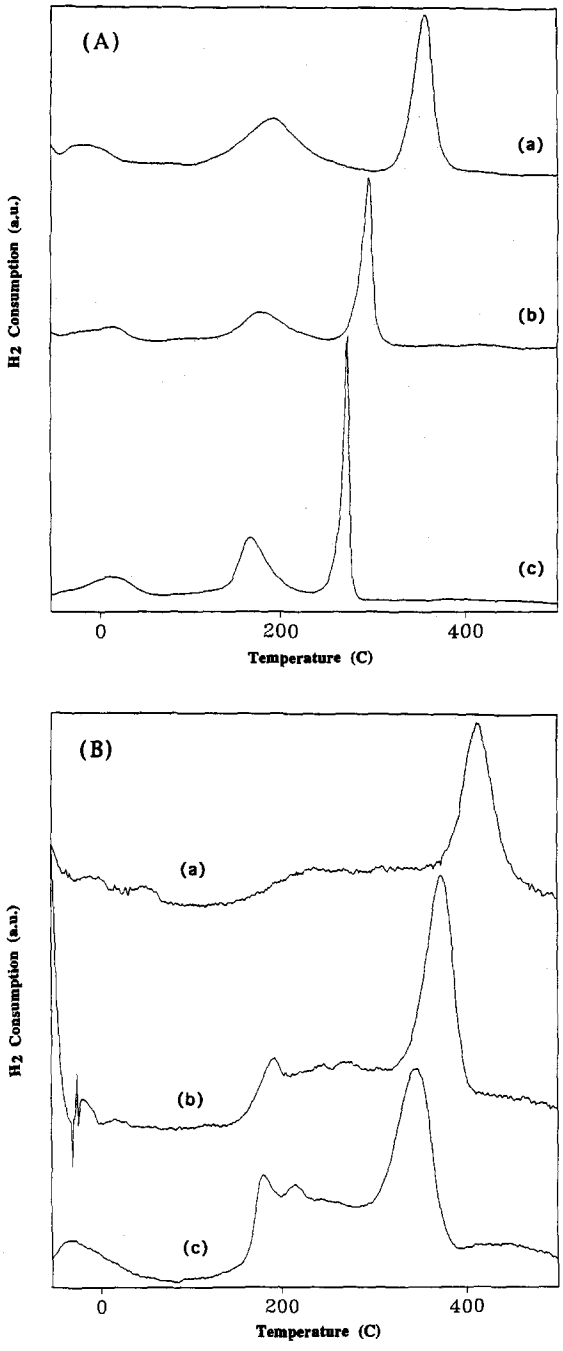

Fig. 1. H_2-TPR of fresh (A) and deactivated (B) Cu/ZSM-5: (a) Cu/ZSM-5-17-68, (b) Cu/ZSM-5-17-102, and (c) Cu/ZSM-5-18-113.

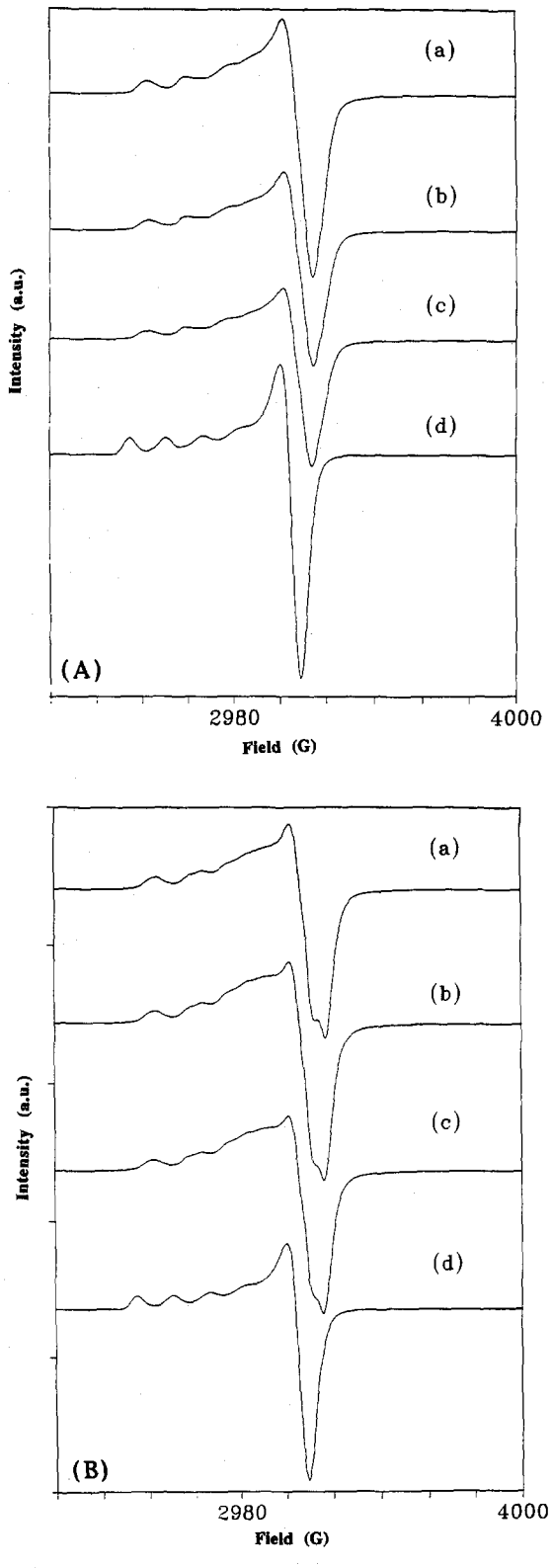

Fig. 2. EPR spectra of fresh (A) and deactivated (B) Cu/ZSM-5: (a) Cu/ZSM-5-17-68, (b) Cu/ZSM-5-17-102, (c) Cu/ZSM-5-18-113, and (d) Cu/ZSM-5-17-68 after exposed to air.

Table 4
EPR intensities of Cu/ZSM-5 and Cu/M/ZSM-5 samples

Sample	Fresh		Deactivated	
	Intensity	Color	Intensity	Color
Cu/ZSM-5-17-68	10.4	light blue	8.9	light blue
Cu/ZSM-5-17-102	7.8	green	9.8	pale blue
Cu/ZSM-5-8-113	7.4	green	8.8	pale blue
Cu/Na-0.5/ZSM-5-17-102 [a]	6.2	gray	5.6	gray
Cu/Na-0.5/ZSM-5-17-102	6.2	gray	4.6	gray
Cu/Ce-0.5/ZSM-5-17-102	11.6	light green	12.0	pale green
Cu/La-0.5/ZSM-5-17-102	8.2	green	9.2	pale green

[a] Treated under dry catalysis conditions at 500°C for 4 h.

and $g_{\|} = 2.26$, were Cu^{2+} ions located in a different coordination environment.

Curves d in Fig. 2A and Fig. 2B are EPR spectra of fresh and deactivated Cu/ZSM-5-17-68 samples after exposed to air (moisture). These EPR spectra were identical, both gave only one type of Cu^{2+} ions with $A_{\|} = 135$ G and $g_{\|} = 2.36$, which can be assigned to hydrated octahedrally coordinated Cu^{2+}. This suggests that after deactivation, the detectable Cu^{2+} ions are still accessible to small molecules, such as H_2O.

The relative intensities of the EPR signals are listed in Table 4. The differences in intensities between fresh and deactivated samples were within experimental error. This means that no Cu^{2+} ions that were highly dispersed in the fresh samples had become EPR silent in the deactivated samples by agglomeration to CuO particles with strong antioferromagnetic coupling.

The XRD patterns of fresh and deactivated Cu/ZSM-5 samples are shown in Fig. 3A and Fig. 3B. No detectable CuO crystallites were observed in any of the three samples. All XRD patterns looked similar, suggesting that no major loss of zeolite crystallinity had occurred. However, the background intensities in the 2θ region between 12 and 24° were noticeably higher in deactivated Cu/ZSM-17-68 and Cu/ZSM-5-17-102 (curves b and c in Fig. 3B), though this was not obvious for the Cu/ZSM-5-18-113 sample (curve c in Fig. 3B). It is possible that, upon deactivation, some amorphous material was formed in the first two samples.

3.2. Cu / M-0.5 / ZSM-5-17-102

In Table 5 the catalytic activities of the modified Cu/ZSM-5 samples are compiled, both before and after deactivation. Modification of the fresh sample by Na, La and Ce did not change the NO reduction activity significantly. The competitiveness factor did not change either, except for the modification with sodium, in which case it was slightly increased. Deactivation increased the competitiveness factor for all samples. However, the rate of deactivation was significantly affected by the modifier. The Na-modified samples deactivated faster, the La-modified sample deactivated slower, whereas the Ce-modified sample deactivated at about the same rate as the unmodified sample. Deactivation was observed for the Na-modified sample even under dry catalysis condition, a condition under which Cu/ZSM-5 did not show deactivation [9].

The TPR profiles of fresh Cu/M-0.5/ZSM-5-17-102 samples are shown in Fig. 4A. The profiles of Cu/ZSM-5 (curve a) and Cu/La-0.5/ZSM-5 (curve d) were similar, whereas those of Cu/Na-0.5/ZSM-5 and Cu/Ce-0.5/ZSM-5 (curves b and c) were different. The Cu/Na/ZSM-5 profile showed a prominent peak at about 145°C and a small peak at about 310°C. The 145°C peak is assigned to the reduction of CuO crystallites to Cu° and the reduction of Cu^{2+} to Cu^{+} [11]. The 310°C peak is assigned to the reduction of Cu^{+} to Cu°, as was done for Cu/ZSM-5 [9]. The Cu/Ce-

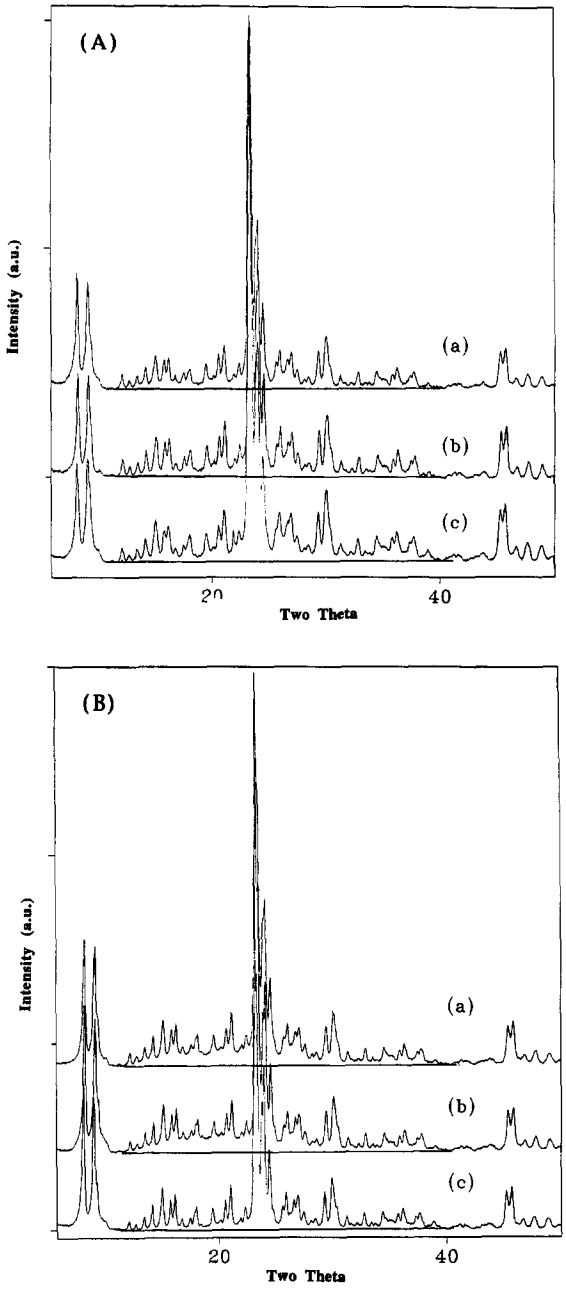

Fig. 3. XRD spectra of fresh (A) and deactivated (B) Cu/ZSM-5: (a) Cu/ZSM-5-17-68, (b) Cu/ZSM-5-17-102, and (c) Cu/ZSM-5-18-113.

0.5/ZSM-5 profile showed a broad band of overlapping peaks over the range of 130–210°C. There was a relatively well-defined peak at 240°C (Fig. 4A, curve c). The ratio of H_2 consumed/Cu was unity for Na and La modi-

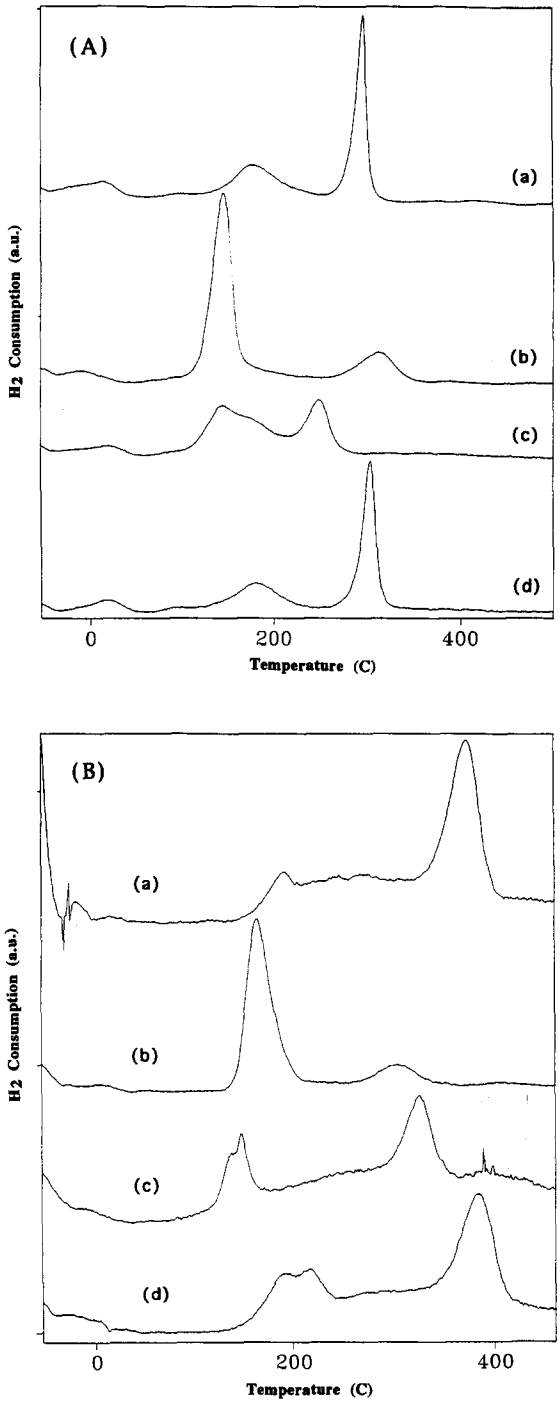

Fig. 4. H_2-TPR of fresh (A) and deactivated (B) Cu/M-0.5/ZSM-5: (a) Cu/ZSM-5-17-102, (b) Cu/Na-0.5/ZSM-5-17-102, (c) Cu/Ce-0.5/ZSM-5-17-102, and (d) Cu/La-0.5/ZSM-5-17-102.

fied samples, but was 1.1 for Ce modified sample, suggesting that some Ce ions were also reduced.

The TPR profiles of deactivated Cu/M/ZSM-5-17-102 samples are shown in Fig. 4B. The profiles of Cu/La-0.5/ZSM-5 and Cu/ZSM-5 were similar. They showed a broad reduction peak at 150–350°C, characteristic of the reduction of copper dispersed in/on Al_2O_3 [9]; and a prominent peak at 370–390°C, due to the reduction of Cu^+ to Cu°. However, the reduction profile of deactivated Cu/Na-0.5/ZSM-5 was similar to that of the fresh sample, no Cu/Al_2O_3 phase was present. The profile of deactivated Cu/Ce-0.5/ZSM-5 showed prominent peaks at 130–160°C and at 325°C, and a broad peak between them. There was also a small peak at about 400°C, which could be the reduction of $CuAl_2O_4$.

The EPR spectra of fresh and deactivated Cu/M-0.5/ZSM-5 are shown in Fig. 5A and Fig. 5B. The spectra c and d in Fig. 5A of fresh Cu/Ce-0.5/ZSM-5 and Cu/La-0.5/ZSM-5 were similar to that of fresh Cu/ZSM-5 (spectrum a in Fig. 5A), showing only one signal for Cu^{2+} ions with $A_{\|} = 154$ G and $g_{\|} = 2.30$. The EPR patterns of the deactivated samples (spectra a, c, and d in Fig. 5B) were also similar, showing two types of Cu^{2+} ions with $A_{\|} = 148$ G, $g_{\|} = 2.31$; and $A_{\|} = 174$ G, $g_{\|} = 2.26$.

The EPR signals of Cu/Na-0.5/ZSM-5 were different from those of the other catalysts. The EPR hyperfine structure of fresh, slightly deactivated (by dry catalysis at 500°C for 4 h) and severely deactivated (by wet catalysis at 500°C for 5 h) samples are shown in Fig. 6. In the fresh sample (curve a), there were three types of Cu^{2+} ions. One, with $A_{\|} = 154$ G and $g_{\|} = 2.30$, was the same as that in a fresh Cu/ZSM-5 sample. The second one, with $A_{\|} = 174$ G and $g_{\|} = 2.26$, was the same as the second type of Cu^{2+} ions present in a deactivated Cu/ZSM-5 sample. The third one gave an even higher $A_{\|}$ and lower $g_{\|}$, although their values could not be determined accurately. This copper species was not present in other modified samples. In a deactivated Cu/Na-0.5/ZSM-5 sample three copper species were detected (curve b in Fig. 5B, and curves b and c in Fig. 6), two of them were similar to those found in a deactivated Cu/ZSM-5. The signal of $A_{\|}$ region of the third Cu^{2+} species overlapped with the second one, but its presence could be seen clearly from the $A_{\perp}$ region (curve b in Fig. 5B).

The relative EPR signal intensities of the Cu/M-0.5/ZSM-517-102 samples are listed in Table 4. The differences between fresh and deactivated samples were relatively small. However, the Cu/Na-0.5/ZSM-5 samples showed a trend of decreasing intensities with increasing

Table 5
Catalytic activities of Cu/M/ZSM-5-17-102 samples [a]

Sample	Fresh			Deactivation time (h) [b]	Deactivated		
	NO conversion to N_2 (%)	C_3H_8 conversion (%)	Competitiveness factor (%)		NO conversion to N_2 (%)	C_3H_8 conversion (%)	Competitiveness factor (%)
Cu/ZSM-5-17-102	49	92	5.3	21	18	23	7.8
Cu/Na-0.5/ZSM-5 [c]	45	75	6.0	4 [c]	37	59	6.3
Cu/Na-0.5/ZSM-5	45	72	6.3	5	16	15	10.7
Cu/Ce-0.5/ZSM-5	48	92	5.2	21	14	21	6.7
Cu/La-0.5/ZSM-5	53	93	5.7	42	24	28	8.6

[a] Activities were obtained under dry catalysis conditions at 400°C (see Experimental).
[b] Time of deactivation conducted under wet catalysis conditions at 500°C (see Experimental).
[c] Treated under dry catalysis conditions at 500°C for 4 h.

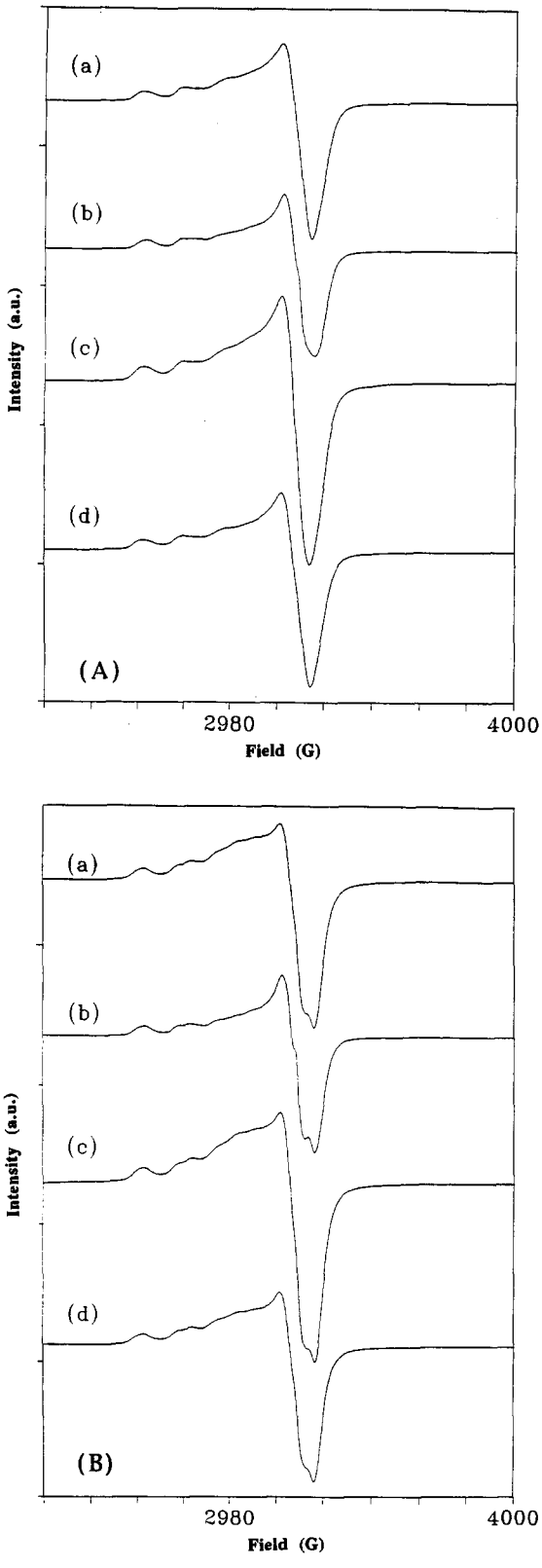

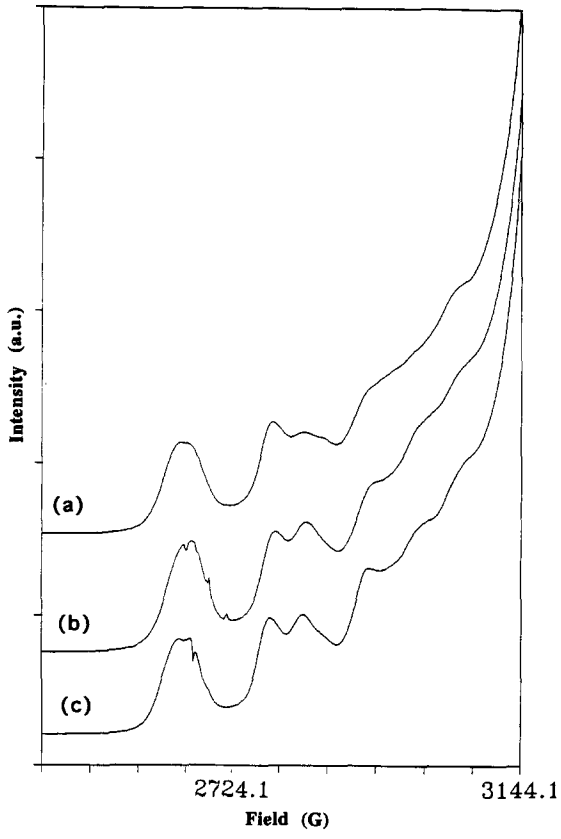

Fig. 6. EPR spectra of Cu/Na-0.5/ZSM-5-17-102: (a) fresh, (b) slightly deactivated (after 5 h dry catalysis at 500°C), and (c) deactivated (after 4 h wet catalysis at 500°C).

extent of deactivation (compare: fresh sample, samples used in 4 h dry catalysis and in 5 h wet catalysis).

The XRD patterns of fresh and deactivated Cu/M-0.5/ZSM-5-17-102 samples are shown in Fig. 7A and Fig. 7B. The pattern of Cu/La-0.5/ZSM-5 (curve d in Fig. 7A) did not show any signs of La_2O_3 or $La_2(CO_3)_3$ crystallites, which suggested that La was well dispersed in the ZSM-5 support. However, CeO_2 crystallites (peaks at 28.8 and 47.8° 2θ) were detected in both fresh and deactivated Cu/Ce-0.5/ZSM-5 (curves c in Fig. 7A and Fig. 7B). CuO crystal-

Fig. 5. EPR spectra of fresh (A) and deactivated (B) Cu/M-0.5/ZSM-5: (a) Cu/ZSM-5-17-102, (b) Cu/Na-0.5/ZSM-5-17-102, (c) Cu/Ce-0.5/ZSM-5-17-102, and (d) Cu/La-0.5/ZSM-5-17-102.

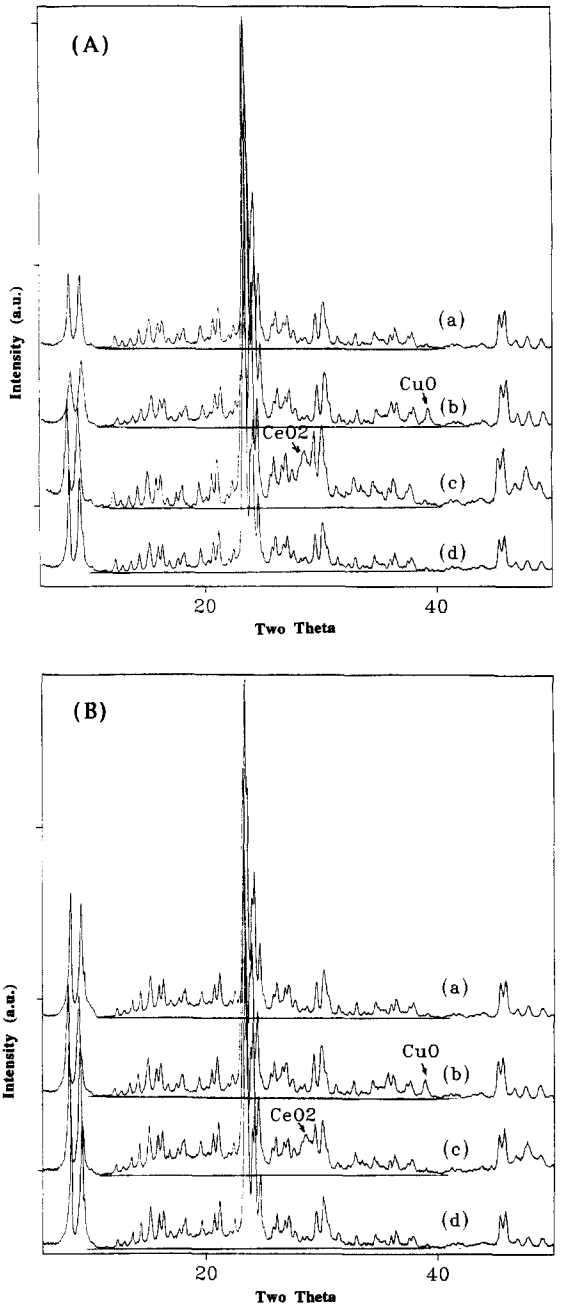

Fig. 7. XRD spectra of fresh (A) and deactivated (B) Cu/M-0.5/ZSM-5: (a) Cu/ZSM-5-17-102, (b) Cu/Na-0.5/ZSM-5-17-102, (c) Cu/Ce-0.5/ZSM-5-17-102, and (d) Cu/La-0.5/ZSM-5-17-102.

lites (peaks at 35.7 and 38.6° 2θ) were detected in both fresh and deactivated Cu/Na-0.5/ZSM-5 (curves b in Fig. 7A and Fig. 7B). Interestingly, CuO crystallites were not detected in Cu/Ce-0.5/ZSM-5. The background intensities in the region at 2θ of 12–24° were substantially increased in the deactivated Cu/ZSM-5 (curve a in Fig. 7B), Cu/Ce-0.5/ZSM-5, and Cu/La-0.5/ZSM-5 (curves c and d in Fig. 7B) samples. This indicated formation of amorphous material in these samples upon deactivation. It is interesting that deactivated Cu/Na-0.5/ZSM-5 (curve b in Fig. 7B) did not show increased background intensity in this region. This suggests that destruction of the zeolite structure was much less severe in this sample than in the other deactivated Cu/M-0.5/ZSM-5 catalysts.

4. Discussion

The results described above show the following trends regarding the deactivation of Cu/ZSM-5 and Cu/M/ZSM-5 catalysts.

(1) Increasing the copper loading up to 113% exchange level (the highest tested) improves the stability of catalyst.

(2) The effect of introducing a second metal ion to Cu/ZSM-5 on the stability depends on the metal ion. La improves the stability, Ce has little effect, and Na has a negative effect.

(3) The nature of the second metal ion has a strong effect on the distribution of the copper species in the catalyst.

(4) The H_2-TPR results indicate that in all deactivated Cu/ZSM-5 and Cu/M-0.5/ZSM-5 catalysts, with the exception of Cu/Na-0.5/ZSM-5, a Cu/Al_2O_3 phase is formed.

These results and those of our previous study [9] can be interpreted on the basis of the general assumption that zeolite protons induce dealumination of the zeolite in the presence of water. Cu^{2+} ions interact with the extracted alumina and form catalytically inactive solids, viz. Cu/Al_2O_3 and/or the spinel $CuAl_2O_4$. In the absence of protons, dealumination is much slower or non-existent. As the total number of

charge compensating ions is defined by the number of Al^{3+} ions in zeolite tetrahedra, it follows that any increase in the number of metal ions, or positively charged oxo-complexes, implies a concomitant decrease in the concentration of zeolite protons.

However, not all metal ions are present in the zeolite with their nominal charge. Hydrolysis of Ce^{3+} ions, for instance, leads to a hydroxide gel, which adsorbs oxygen and is dehydrated to CeO_2 upon calcination:

$$Ce^{3+} + 3H_2O = Ce(OH)_3 + 3H^+ \quad (1)$$

$$2Ce(OH)_3 + \frac{1}{2}O_2 = 2CeO_2 + 3H_2O \quad (2)$$

CeO_2 does not compensate negative charges of the zeolite lattice and therefore does not lower the proton concentration. The original protons replaced by Ce^{3+} during Ce introduction, are regenerated upon the complete hydrolysis of Ce^{3+} [Eq. (1)].

Increase of the copper loading does improve the stability of Cu/ZSM-5. Since two of the three prevailing Cu species, Cu^{2+} and [Cu-O-Cu]$^{2+}$, carry a positive charge, an increase in their concentration implies a decrease in the proton concentration on exchange sites. As a consequence, the rate of dealumination and catalyst deactivation is lowered substantially.

The TPR results show that introducing La to Cu/ZSM-5 does not change the distribution of the Cu species, while it does improve the catalyst stability. The XRD results show that La is fairly well dispersed in the sample. These data are consistent with the hypothesis that La, like excess Cu, basically operates by reducing the proton concentration. Indeed, inhibition of the dealumination of Y zeolite under hydrothermal treatment by ion-exchanged La is well known. We refer to papers by Li et al [12], and Maugé et al [13], and the references quoted therein. With H_2O in feed, La^{3+} undergoes hydrolysis to form $La(OH)^{2+}$ [12] or T-O-La-$(OH)_2$-La-O-T (T = Si, Al) dimers [13]. Since ZSM-5 has a much higher Si/Al ratio than Y zeolite, exchange sites are relative far away from each other, and Coulomb interaction will favor formation of mono-charged $La(OH)_2^+$ or LaO^+. Hydrolysis thus leads to the formation of La oxo-complexes with positive charge, which, again, will lower the concentration of zeolite protons in ZSM-5, and by consequence, retard the dealumination under the lean NO_x reduction conditions.

The effect of excess Na on catalyst stability is more complicated. As mentioned, impregnation of Na oxalate accelerates the deactivation of Cu/ZSM-5. As excess Na is expected to lower the concentration of protons, one would expect suppression of zeolite dealumination, as was indeed observed by Suzuki, et al [14]. In accordance with their result, both the present TPR and XRD results show that deactivation of Cu/Na-0.5/ZSM-5 was not accompanied by dealumination of ZSM-5 or formation of inactive Cu/Al_2O_3. It follows that the deactivation of Cu/Na-0.5/ZSM-5 must have a different cause.

The possibility that CuO crystallites present in Cu/Na-0.5/ZSM-5 block pores and thus make the reaction diffusion controlled is not very likely. The copper loading in the present samples is relatively low and the exchange sites are well accessible through numerous pathways in the three dimensional channel structure of ZSM-5 support. Moreover, formation of CuO particles in the Na rich samples after calcination in O_2 at 500°C for 2 h have been detected by XRD; however, the initial NO reduction activity was not obviously lower than that of unmodified Cu/ZSM-5. Also, the possibility that the deactivation of the Na rich samples is due to excessive coking has been rejected, since the catalytic activity can not be regenerated by recalcination of the used sample.

One cause of the lower activity of some Na-rich samples is complete hydrolysis of Cu^{2+} to $Cu(OH)_2$ and, upon dehydration, formation of catalytically inactive and EPR silent CuO

clusters. For the sample with very high Na concentration (150% nominal exchange level), the formation of CuO after calcination was complete and no isolated Cu^{2+} ions were left in ZSM-5, as shown by H_2-TPR, EPR and XRD [9]. This Cu/Na-1.5/ZSM-5 indeed did not show any NO reduction activity under the usual reaction conditions. Clearly, the formation of inactive CuO particles is promoted by addition of Na, and is one important cause of the lower activity.

This may explain, partly, why a smaller excess of Na results in a catalyst which is initially quite active, but deactivates severely over several hours. The EPR intensities of Cu^{2+} (Table 4) show a decreasing trend from fresh unmodified Cu/ZSM-5-17-102 (relative intensity = 7.8) to fresh Cu/Na-0.5/ZSM-5 (intensity = 6.2), to slightly deactivated Cu/Na-0.5/ZSM-5 by dry catalysis for 4 h (intensity = 5.6), and to severely deactivated Cu/Na-0.5/ZSM-5 (intensity = 4.6). The EPR intensity loss suggests that more and more EPR silent CuO particles are formed, and this agglomeration of active Cu^{2+} ions to inactive CuO particles is one of the reasons for Cu/Na-0.5/ZSM-5 deactivation. However, the fact that the extent of the formation of inactive CuO particles is less than the 70% loss of NO conversion activity (comparing the fresh Cu/ZSM-5-17-102 and the highly deactivated Cu/Na-0.5-17-102 in Table 5), suggests that formation of inactive CuO crystallites is only partly contributing to the deactivation of Cu/Na-0.5/ZSM-5.

The EPR data suggest an additional cause for the deactivation of Cu/ZSM-5. The EPR spectrum reveals that the isolated Cu^{2+} ions exist in at least two different coordination environment in all of the deactivated Cu/(M-0.5/)ZSM-5. One of these (with $A_{\|} = 154$ G and $g_{\|} = 2.30$) is present in both active and used Cu/Na-0.5/ZSM-5. The second one (with $A_{\|} = 174$ G and $g_{\|} = 2.26$) represents only a small fraction of the Cu^{2+} in the fresh Cu/Na-0.5/ZSM-5, but is the dominant species in the deactivated sample. These suggest that Cu^{2+} ions migrate to a different coordination environment upon deactivation. Kucherov et al. observed Cu^{2+} in two different coordination environment even in the fresh Cu/H(Na)-ZSM-5-34.5-20 samples [15]. We did not observe the EPR signal with $A_{\|} = 174$ G and $g_{\|} = 2.26$ in our fresh catalysts. It appears that in our samples, the appearance of the second copper ions only occurs during extensive exposition of the catalyst to the reaction gases with steam, as shown in all three deactivated Cu/ZSM-5 samples; or when Na is added to Cu/ZSM-5 sample. As migration of metal ions through intact zeolite channels is known to be very fast at temperatures above 200°C, it is unlikely that the new Cu^{2+} species is simply due to migration of Cu^{2+} ions through the channels of a rigid zeolite. Rather, the present data suggest that some solid state reaction with a rather high activation energy may be responsible for the formation of the new coordination environmental sites, and the migration of Cu^{2+} ions to these new sites during the deactivation of Cu/Na-0.5/ZSM-5 or Cu/ZSM-5 samples lead to the further loss of activity.

In all catalysts studied, deactivation increases the competitiveness factor (Tables 3 and 5); that is, the hydrocarbon is used more efficiently to reduce NO to N_2. There are at least two contributions to this effect. First, the competitiveness factor of a catalyst is generally higher if the conversion is lower. Second, deactivation may cause a greater loss of hydrocarbon combustion sites than NO reduction sites. At present, our data can not distinguish between these possibilities.

5. Conclusion

For the purpose of stabilizing Cu/ZSM-5 under the lean NO_x reduction condition, increasing copper loading and introduction of La ions can decrease the population of proton exchanged sites, and, hence, retard the dealumination and deactivation rate. In contrast, introduction of Ce does not affect the stability because

Ce^{3+} ions are completely hydrolyzed and CeO_2 crystallites are formed upon calcination. Introducing excess Na has a negative effect on the stability because Na^+ ions promote the hydrolysis of Cu^{2+} ions to form inactive CuO particles; in addition, part of the Cu^{2+} ions migrate to sites with a different coordination environment.

The importance of dealumination on the deactivation of Cu/ZSM-5 catalysts is further confirmed by samples of different copper loadings. An increase of the concentration of charged copper species, Cu^{2+} or $[Cu\text{-}O\text{-}Cu]^{2+}$ ions, results in a concomitant decrease of the concentration of zeolite protons, and consequently prevent the detrimental action of the zeolite dealumination and the formation of Cu/Al_2O_3.

Acknowledgements

We thank B.J. Adelman for providing the Cu/ZSM-5-18-113 sample. Support of this work by the Ford Motor Corporation and the Engelhard Corporation is gratefully acknowledged.

References

[1] M. Iwamoto, H. Yahiro, S. Shundo, Y. Yu-U and N. Mizuno, Shokubai (Catalyst), 32 (1990) 430.
[2] W. Held, A. Konig, T. Rihter and L. Ruppe, SAE Paper, 900496 (1990).
[3] C. Bartholomew, R. Gopalakrishnan, P.R. Stafford and J.E. Davison, AIChE 1992 Annual Meeting, Paper no. 240a.
[4] D.R. Monroe, F.A. Matekunas, C.L. Dimaggio and D.D. Beck, General Motors Research Publication, GMR-7799 (1992).
[5] R.A. Grinsted, H.W. Jen, C.N. Montreuil, M.J. Rokosz and M. Shelef, Zeolite, 13 (1993) 602.
[6] K.C.C. Kharas, H.J. Robota and D.J. Liu, Appl. Catal. B, 2 (1993) 225.
[7] S. Matsumoto, K. Yokota, H. Dio, M. Kimura, K. Sekizawa and S. Kasahara, Catal. Today, 22 (1994) 127.
[8] T. Tanabe, T. Iijima, A. Koiwai, J. Mizuno, K. Yokota and A. Isogai, Appl. Catal. B, 6 (1995) 145.
[9] J. Yan, G.-D. Lei, W.M.H. Sachtler and H.H. Kung, submitted.
[10] M. Iwamoto, H. Yahiro, N. Mizuno, W. Zhang, Y. Mine, H. Furukawa and s. Kagawa, J. Phys. Chem., 96 (1992) 9360.
[11] T. Beutel, J. Sárkány, G.-D. Lei, J.Y. Yan and W.M.H. Sachtler, J. Phys. Chem., in press.
[12] O. Li, L. Dai, J. Xiong, L. Zhu and Z. Xue, Zeolites, 14 (1994) 367.
[13] F. Maugé, P. Gallezot, J.-C. Coucelle, P. Engelhard and J. Grosmangin, Zeolites, 6 (1986) 261.
[14] K. Suzuki, T. Sano, H. shoji and T. Murakami, Chem. Lett., (1987) 1507.
[15] A.V. Kucherov, A.A. Slinkin, D.A. Kondrat'ev, T.N. Bondarenko, A.M. Rubinstein and Kh.M. Minachev, Zeolites, 5 (1985) 320.